Fermi National Accelerator Laboratory

FERMILAB-Pub-87/186-E
[E-741/CDF]

Radial Wire Drift Chambers for CDF Forward Tracking*

M. Atac, G. W. Foster, C. Newman-Holmes
A. Para, J. Patrick, M. Sekiguchi, G. P. Yeh
Fermi National Accelerator Laboratory
P.O. Box 500, Batavia, Illinois 60510

J. Bellinger, D. Cline, N. K. Mondal, R. Markeloff, J. Rhoades
University of Wisconsin
Madison, Wisconsin 53706

F. Feyzi
Physical Sciences Laboratory
University of Wisconsin
Stoughton, Wisconsin 53589

July-August 1987

*Submitted to Nucl. Instrum. Methods A

RADIAL WIRE DRIFT CHAMBERS FOR CDF FORWARD TRACKING

M. Atac, G. W. Foster, C. Newman-Holmes,

A. Para, J. Patrick, M. Sekiguchi, G. P. Yeh

Fermi National Accelerator Laboratory[1], Batavia, IL

J. Bellinger, D. Cline, N. K. Mondal, R. Markeloff, J. Rhoades

University of Wisconsin, Madison, WI

F. Feyzi

Physical Sciences Laboratory, Stoughton, WI

May 14, 1987

Abstract

We describe the design, construction, and operating experience of unique drift chambers with radially strung wires for the Collider Detector of Fermilab (CDF) [1] which cover forward and backward cone angles between 2° and 10° and 170° to 178°. The chambers are capable of operating in our high rate and high track multiplicity environment with excellent multitrack resolution of 2-3 mm and high tracking accuracy of 140 μm per wire. Results from the recent running experience will be presented.

[1]Operated by Universities Research Association under Contract with the U.S. Department of Energy No. DE-AC02-76CH03000

1. Description of the Chambers

The forward tracking chambers (FTC) or "radial wire drift chambers," were built to cover the forward/backward regions between 2° and 10° in θ (about 2 units of rapidity) as shown in Fig. 1. The 72 wedge shaped cells of an FTC are shown in Fig. 2. The chamber contains planes of anode and field shaping wires that alternate with planes of cathode strips. The wire planes and cathode planes of each 5° cell are slanted at 2° relative to the beam axis so that left-right ambiguities can be resolved by demanding that tracks point back to the vertex. The anode plane has 21 active, 50 μm diameter sense wires and 26 field shaping wires (150 μm in diameter that are strung approximately along the radial direction (normal to the beam axis). Thus the drift spacing varies from a minimum of 5.4 mm at r = 12.5 cm to a maximum of 28.3 mm at a radius of 72.5 cm (see Fig. 3). Time over threshold information from the sense wires is read out using LRS 1879 multihit TDC's. Two of the sense wires (the Stablohm 800, Cr-Ni-Al-Cu alloy) [2]) are instrumented with 30 MHz FADC's for current division so that an R-ϕ-Z measurement can be made for each track. There are a total of 2736 active sense wires in the forward and backward directions.

The cathode planes are made of 125 μm thick G10 sheets with 6 mm wide, 125 μm thick aluminum strips on each side. This allowed the cathode voltage to be graded along the sheets to account for the widening of the cell with radius. A very small (1 mm wide, 3 mm long, 0.25 mm thick) surface mount resistor is silver epoxied between the strips to provide for the resistive voltage divider network. There are 84 strips on each side of a cathode plane, and there is about a 30 volt

drop between each pair of strips under standard running condition.

Care was taken to minimize the mass of the FTC. The end plates, which carry the load of the wire and cathode plane tensions between the inner and outer cylinders, are of a carbon-fiber/Hexcell laminate [3] The inner cylinder is a 250 μm thick aluminum, 12 mm thick Rohacell [4] foam sandwich. The outer cylinder is masked by the plug calorimeters and, since its mass is not a concern, is constructed of 8 mm thick aluminum. The inner and outer cylinders have 3.1 mm diameter wire positioning holes located to better than 12 μm precision by a computer controlled machine [5]. The wire feed-throughs are injection molded Noryl (polyphenylene oxide with polystyrene made by General Electric Co.) with stainless steel crimp tube inserts. The wires were crimped in place under 40 gram tension by a special crimping tool. The Noryl feed-throughs are found to be excellent in mechanical and electrical properties [6].

The field shaping cathode planes have about 2.5 kg of tension applied diagonally from each corner using piano wires going through small holes on the inner and outer cylinders. This provides a longitudinal force and a substantial transverse force which keep the planes flat to within 250 μm for the horizontal cells.

The average radiation length of materials in the structure described above for tracks from the interaction point regions are given in Table 1 below:

Table 1:

Angular Region	Type of Material	Radiation Length
I ($1.8^\circ - 2^\circ$)	Graphite-Hexcell	0.012
	Aluminum-Rohacell	0.16
	Noryl Feed-through	0.02
II ($2^\circ - 10^\circ$)	Graphite-Hexcell	0.012
	Cathode Sheet	0.03

The FTC's are built in two halves so that the halves can be moved apart on rails which open the 10° plug hole for servicing the inner part of the CDF. This caused considerable difficulty in construction. Fig. 4 shows a view of the inner cylinder with feed-throughs and crimp tubes, a part of the wiring, and the inner sections of the cathode strips. We also see the carbon fiber-Hexcell support plates and the top and bottom covers.

Some of the mechanical specifications of the FTC's are summarized in Table 2 below:

Table 2: Some Mechanical Specifications

Outer Radius:	72.5 cm
Inner Radius:	12.5 cm
Wire Length of Sensitive Volume:	60 cm
Minimum Drift Distance:	5.4 mm
Maximum Drift Distance:	28.3 mm
Sense Wire:	50 μm gold plated tungsten and
	50 μm Stablohm (for current division)
Field Wire:	150 μm stainless steel 304
Cathode Strips:	25 μm thick 6 mm wide on 125 μm G10
Total Number of Wires:	6768
Total Number of Sense Wires:	2736
Wire Tension:	40 gram
Cathode Plane Tension:	2.5 kg (each)
Chamber Volume:	0.5 m^3 (total volume 2 m^3)

The chambers were run with equal portions of Argon/Ethane flowing through isopropyl alcohol (2-propanol) at $-1.1°C$ adding about 0.8% vapor to the premixed gas by volume. This gas mixture was selected after extensive research on wire chamber aging [7]. The gas flow rate for one-half unit chamber was 0.5 liter per hour.

Fig. 5 shows the two halves of the chambers before mounting on the plug. It shows the two halves of the inner cylinder that go around the beam pipe, the

cover cathode planes, and a circular array of quartz windows for laser beam studies of each cell. A nitrogen UV-laser was used for studying drift chamber parameters for various cells. Fig. 6 shows the two halves of the chambers on the plug in open position around the 10° forward cone.

2. Electronics

Fig. 7 shows a block diagram of the FTC data acquisition system for one wire. All preamplifier cards are kept within the chamber enclosure and located on the periphery of the outer cylinders. where they are shielded by the calorimetry. Each preamplifier card which contains 21 circuits is directly attached to the aluminum body that is used as the common ground for each chamber. All coaxial cable shields are soldered to this common ground system. Each wire was connected to the corresponding preamplifier through a high voltage decoupling capacitor. Each amplifier board distributes a common positive high voltage to the sense wires from a bus strip. All high voltage bus lines to the sense wires, the field wires, and the cathode planes are kept within the common gas enclosure of Argon/Ethane/isopropyl alcohol to eliminate surface corona that may occur due to humidity.

Signals from each sense wire are preamplified by a surface mount hybrid circuit (originated by V. Radeka, Brookhaven National Lab) which was mass produced [8] after a small modification. The preamplifier has a rise time of 1.2 ns, a decay time of 32 ns, and a charge gain of 160 with an input equivalent noise of 3000 electrons into a 10 pf capacitor. The output signals are carried to hermetically sealed multipin connectors attached to the chambers via 1 mm diameter custom made 56 Ω coaxial cables and from there to the amplifier-shaper-discriminator (ASD) boards

using 3 m lengths of the same type cable. A preamplifier gain uniformity of 4% was achieved by on-line laser trimming during the production.

The outputs from the preamplifiers are further amplified by a factor of 20, pulse shaped and discriminated by the ASD circuits, Fig. 8. The pole zero filtering circuit after the transistor Q_1 considerably narrows the tail of the pulses. The full widths of the pulses for minimum ionizing tracks were less than 20 ns during the running conditions. A 60 m long flat ribbon cable [9] carries the differential outputs from the LeCroy MVL407 discriminators to the LeCroy 1879 FASTBUS TDC boards which are kept in the counting room. The TDC's were run with better than 1 nsec least bit accuracy with a full scale of 1 μsec.

Analog outputs from Q_3 emitter followers are further amplified and shaped for current division using 30 MHz Flash ADC's. The outputs were very useful for monitoring signal to noise and amplifier gains.

Two wires of each 5°-sector were instrumented for current divison to obtain two R-ϕ-Z coordinates using 30 MHz FADC's. The Stablohm wires of every other cell were jumpered in the inner cylinder compartment, and currents were measured from outer ends of the wires. This way the amount of material in the way of tracks was minimized, and more optimal resistance ($\sim 800\,\Omega$) was obtained for the current division measurements. A full description of the FADC system is given in Ref. [10].

3. Laboratory Tests

Some early tests were carried out using the first production chamber. A nitrogen UV-laser was used for the tests [11]. The laser beam of $\sim$ 180 microjoule intensity that was collimated to 400 μm full width entered one of the 5° cells through

a quartz window shown in Fig. 5 to ionize the chamber gas. The gas mixture for these tests was 49.6% Argon - 49.6% ethane - 0.8% ethanol and the applied high voltages were: +1850 V on the sense wires - 400 V on the field wires, and -400 V to -3100 V on the cathode planes. This gas mixture was abandoned after these early tests when the aging effect [6] by the gas on the Stablohm wires was discovered. Then as mentioned earlier, an Argon-Ethane-isopropyl alcohol mixture was used for the $\bar{p}p$ collider runs.

The 337 nm wavelength UV-beam produced sufficient primary electrons in the gas. There was no need to add a low ionization potential gas component into the mixture. This may be due to ethanol's high UV-absorption cross section for this wavelength. UV-beam tracks were reconstructed using 21 wire hits and residuals from the linearily fitted tracks were calculated. Fig. 9 shows the residuals for the wires 13 and 14 around the resolution minimum. The drift time to drift distance relation is very linear as seen in Fig. 10. The laser beam was moved relative to the chamber with 10 micron precision for the measurements. The single wire $\sigma_{\rm rms}$ of the residuals was computed at each beam position. Fig. 11 shows the expected behavior of $\sigma_{\rm rms}$ as a function of the drift distance. The average $\sigma_{\rm rms}$ is around 80 μm.

Single wire residuals were also measured using cosmic rays. Fig. 12 shows the residuals for wires 9 and 10. The $\sigma_{\rm rms}$ was found to be around 110 μm. This is an average value for the entire cell for cosmic ray tracks at wide range of angles.

The considerably better resolution obtained with UV tracks is most probably due to the fact that the primary electrons are produced at rest by the UV-beam,

and drift chamber pulses are more uniform in shape than the pulses produced by the minimum ionizing tracks, thus minimizing time slewing effects.

4. Chamber Gas

As mentioned earlier there was a systematic study of the drift chamber gas for long term aging effects on the wires and the cathode planes and the study of the electron drift velocity properties of the gases [12]. The Argon-ethane-2-propanol gas mixture has produced very long lifetimes even for the Stablohm wires which are used for the current division measurements. A specially designed bubbler with a heat exchanger to precool the gas and a commercial refrigerator were used. The temperature stability of the cooler was within 0.1°C for the entire four month $\bar{p}p$ data collection period.

The drift velocity was found to be well saturated above electric fields of 900 V/cm field and independent of the 2-propanol addition within -1°C to -9°C cooler temperatures (Fig. 13). A specially designed drift chamber [12] and the laser beam were used for the measurements.

5. pp Runs

All four halves of the forward tracking chambers were used for taking data during four months of proton-antiproton collisions at 1.8 TeV (center of mass). At these energies, there are about 15 charged particles on the average in both directions. About 20-30% of the tracks may be due to interacting secondaries from the material around the 10° cone, beam pipe, and vertex time projection chambers [10]. The chambers ran well during the period. They performed better as they were

used. The average beam off current drawn by groups of 156 sense wires was less than 50 nanoamperes. There were occasional HV power supply trips due to beam spray when the Tevatron quenched or the $\bar{p}p$ beam was dumped, but there were no broken wires out of a total of 6768 wires. A few of the 150 μm thick stainless steel field wires and two of cathode sheets with aluminum strips were found to be loose. For those sections either the HV was turned down or kept off until the end of the run.

The running voltages of the chambers were +1750 V on the sense wires, -300 V on the field wires, and -3100 V maximum voltage on the cathode planes. This produced a gas gain of $\sim 6 x 10^3$. The gain was purposely kept low to have good multitrack resolution.

The TDC's are capable of measuring leading edges and the trailing edges of the pulses, thus providing pulse width measurements. Fig. 14 shows the pulse width distribution for linearly fitted tracks that originate from the $\bar{p}p$ collision vertices. The distribution looks very much like a Landau distribution. This is expected since the measured pulse width is dependent on the pulse height. We see in the figure that the average pulse width is around 34 nanoseconds which corresponds to 1.5 mm in electron drift distance. Fig. 15a and b show double and triple tracks in a cell, respectively. The double tracks are plotted with the corresponding pulse widths. We are convinced that double tracks can be identified if they are separated by at least 1 mm. This capability is important to identify closely spaced Dalitz pairs or π^o conversion electrons in the material preceding the forward electromagnetic calorimeters.

Line fits to the leading edge of the tracks in the figures indicate good tracking accuracy. Fig. 16 shows single wire residuals averaged over all wires for the tracks originating from the vertex regions. The distribution is gaussian with $\sigma_{\rm rms} = 140\,\mu$m resolution. There was no drift velocity correction made for the plot. It indicates that the electron drift velocity is well saturated in the entire space of the cell. Most of the tracks were found to be free of electronic noise.

The data from current division using the FADC's need to be carefully analyzed with individual wire amplifier gain calibration; thus these data will not be reported at this time. Early measurements using a single wire gave results better than $\sigma_{\rm rms} = 1$ cm.

6. Conclusions

Radial wire drift chambers have been built and successfully operated in a high multiplicity environment. The chambers worked well and have good ϕ resolution. There were no broken wires or measurable degradation after a total integrated flux of $10^8 - 10^9$ charged particles going through each chamber. A few low tension field wires and cathode planes were found. These will be corrected before the next running period.

Acknowledgments

The authors express their appreciation to P. Bloom, J. Lins, and D. Grim for wiring the chambers; to L. Thomas and T. Winch for various discussions on construction; and the Physical Sciences Laboratories Machine Shop Staff for their contributions; to Dr. R. Kadel, M. Hrycyk, and J. Kowalski for the crimp tools; to

Ayfer Atac for her creative drawings; to A. King for his contributions on the power supplies and ASD boards; to R. J. Yarema for his advice on the preamplifiers; to Drs. A. Tollestrup, R. Schwitters, and D. Theriot for very useful discussions; and to Dr. K. Kondo for his support by providing the FADC system.

References

[1] F. Abe et al., "The Collider Detector at Fermilab," submitted to Nucl. Instrum. and Methods.

[2] Stablohm Wire, Cr-Ni-Al-Cu alloy, manufactured by California Fine Wire Company.

[3] Manufactured by Hexcell Company, California.

[4] Manufactured by Roehm and Haas Company, West Germany.

[5] Trace-A-Matic Company, Brookfield, Wisconsin.

[6] M. Atac, IEEE Trans. on Nucl. Sci., Vol. NS-31, No. 1 (1984) 99.
J. Kadyk, "Proc. of the Workshop on Radiation Damage to Wire Chambers."
M. Atac, Proc. of the Workshop on Radiation Damage to Wire Chambers."

[7] M. Atac, IEEE Trans. on Nucl. Sci., Vol. NS-34, No. 1, Feb. 1987, 476.

[8] Centralab Inc., Milwaukee, Wisconsin.

[9] T&B Ansley Company, Los Angeles, California.

[10] F. Snider et al., to be published in Nucl. Instrum. and Methods in Physics Research.

[11] M. Atac, T. Hessing, and F. Feyzi, IEEE Trans. on Nucl. Sci., Vol. 33, No. 1 (1986) 189.

[12] M. Atac, W. Coleman, T. Hessing, R. W. Kadel, M. Pratt, and R. L. Wagner, Nucl. Instrum. and Meth. in Phys. Research, A249 (1986) 265.

Figure Captions

Fig. 1 Cross section view of CDF.

Fig. 2 An isometric veiw of the radial wire drift chamber configuration.

Fig. 3 A beam view of a radial cell.

Fig. 4 A photograph of the inner cylinder showing the feed-throughs, crimp tubes, a part of the wiring, inner sections of the cathode strips, and carbon fiber-Hexcell support plates.

Fig. 5 A photograph of two halves of one unit after completion, showing the inner cylinder sections that go around the beam pipe, the cover cathode planes, connectors, and the quartz windows for the laser beam studies.

Fig. 6 A photograph of the chambers on the end-plug in an open position around the 10° cone.

Fig. 7 A block diagram of the FTC data acquisition system for one wire.

Fig. 8 A circuit diagram of the amplifier-shaper-discriminator (ASD).

Fig. 9 Residual distributions for linearly fitted tracks using the nitrogen UV-laser beam.

Fig. 10 Space-time relation using the laser beam.

Fig. 11 Resolution as a function of the electron drift space.

Fig. 12 Residuals distribution for linearly fitted tracks using cosmic-rays.

Fig. 13 Electron drift velocity as a function of the electric field in the gas mixture of equal portions of argon and ethane bubbling through 2-propanol at different refrigerator temperatures measured with single cell drift chamber.

Fig. 14 A pulse width distribution for linearly fitted tracks originating from $\bar{p}p$ collision vertices. The pulse widths were measured by LeCroy 1879 FASTBUS TDC's using trailing edge and leading edge time differences. It is like a Landau distribution as expected.

Fig. 15a Two tracks from a $\bar{p}p$ collision which appear in one cell.
The pulse widths and fits to leading edge times fittings are shown.

Fig. 15b Three tracks in a cell originating from a $\bar{p}p$ collision vertex.
A fit to leading edge times is shown.

Fig. 16 The residuals distribution for all wires using a $\bar{p}p$ run.
Tracks originating from the vertex were selected.

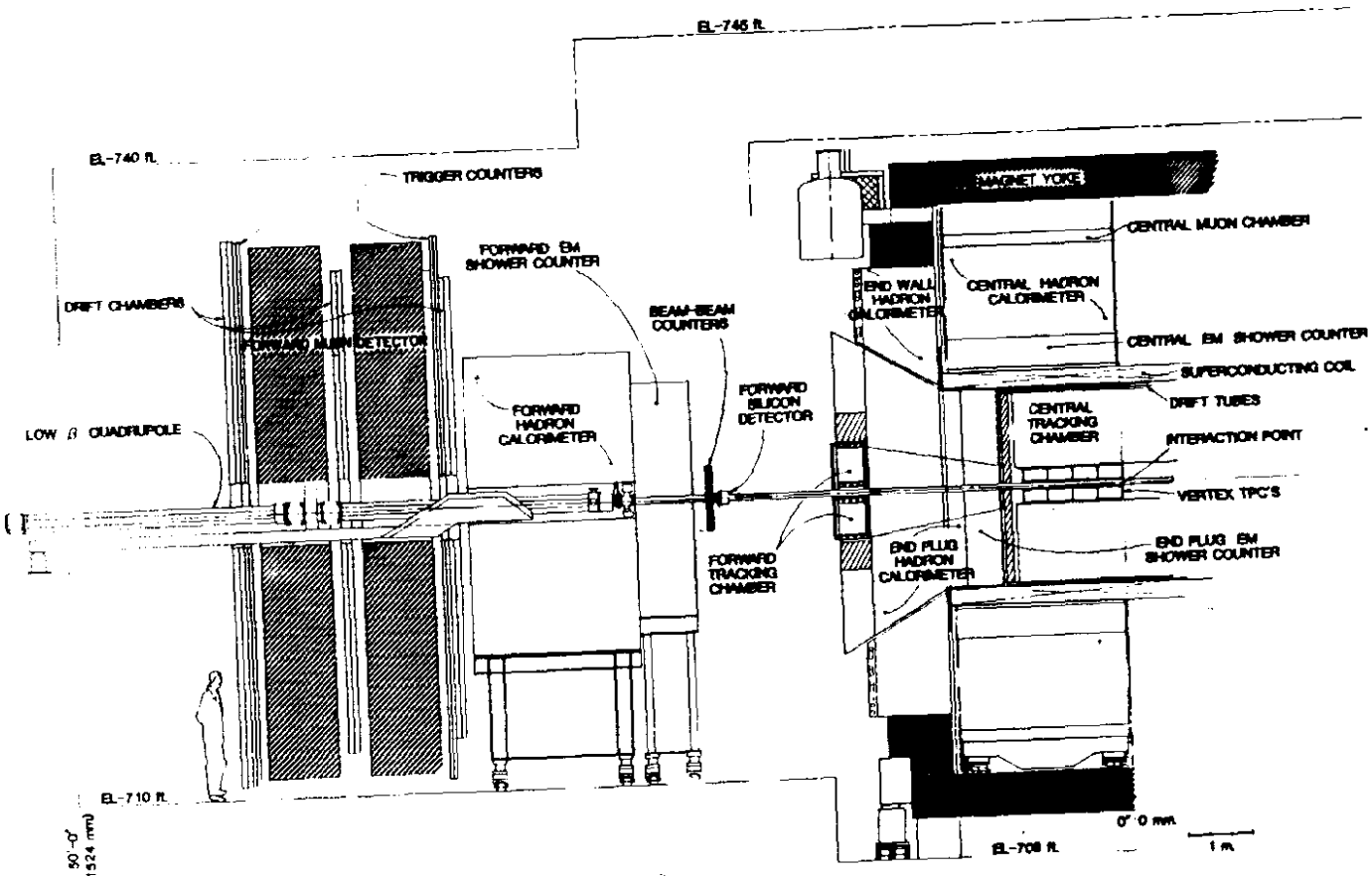

ELEVATION VIEW LOOKING SOUTH

Fig. 1

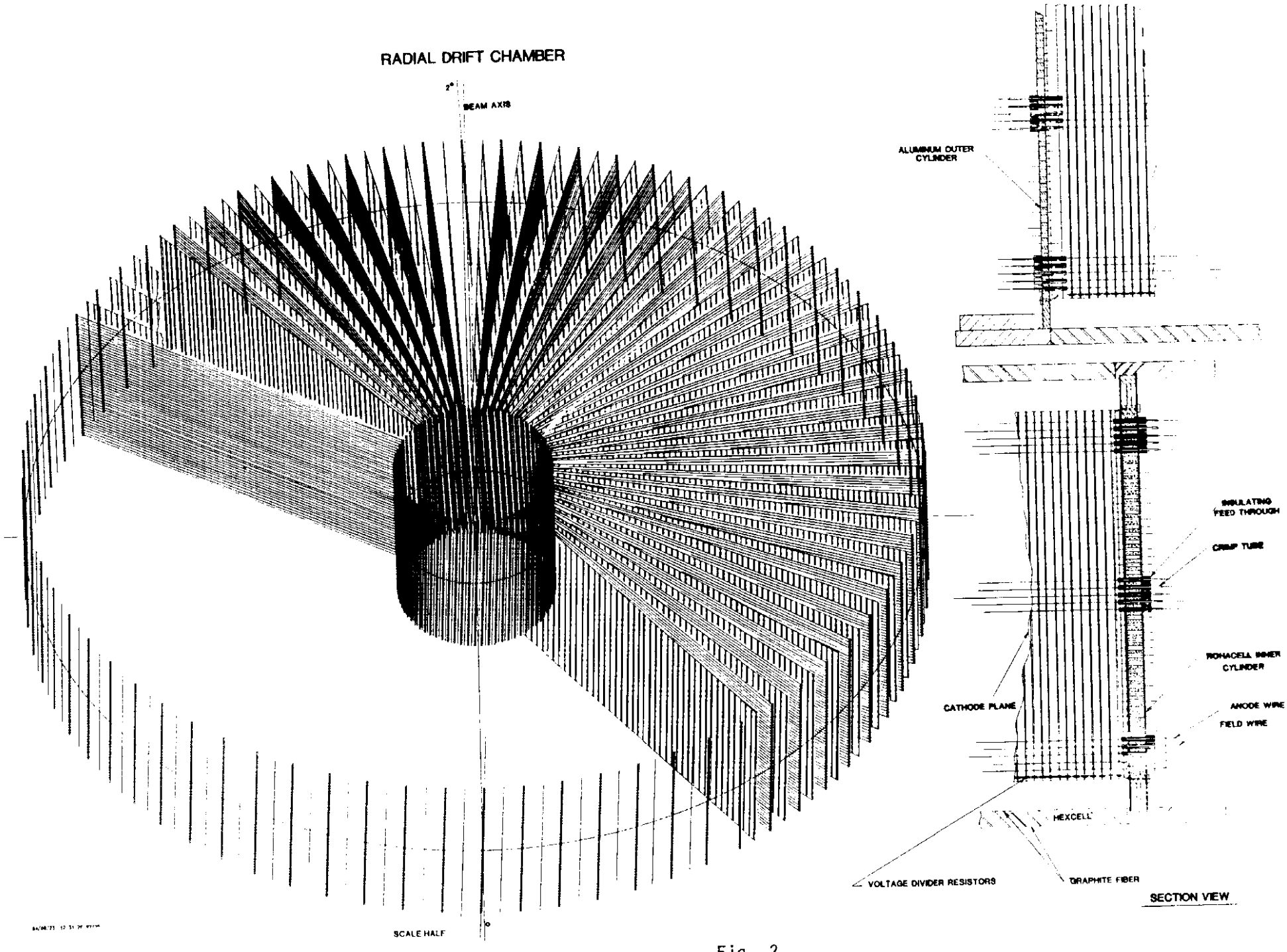
RADIAL DRIFT CHAMBER
BEAM AXIS
SCALE HALF
ALUMINUM OUTER CYLINDER
INSULATING FEED THROUGH
CRIMP TUBE
RONACELL INNER CYLINDER
CATHODE PLANE
ANODE WIRE
FIELD WIRE
HEXCELL
VOLTAGE DIVIDER RESISTORS
GRAPHITE FIBER
SECTION VIEW

Fig. 2

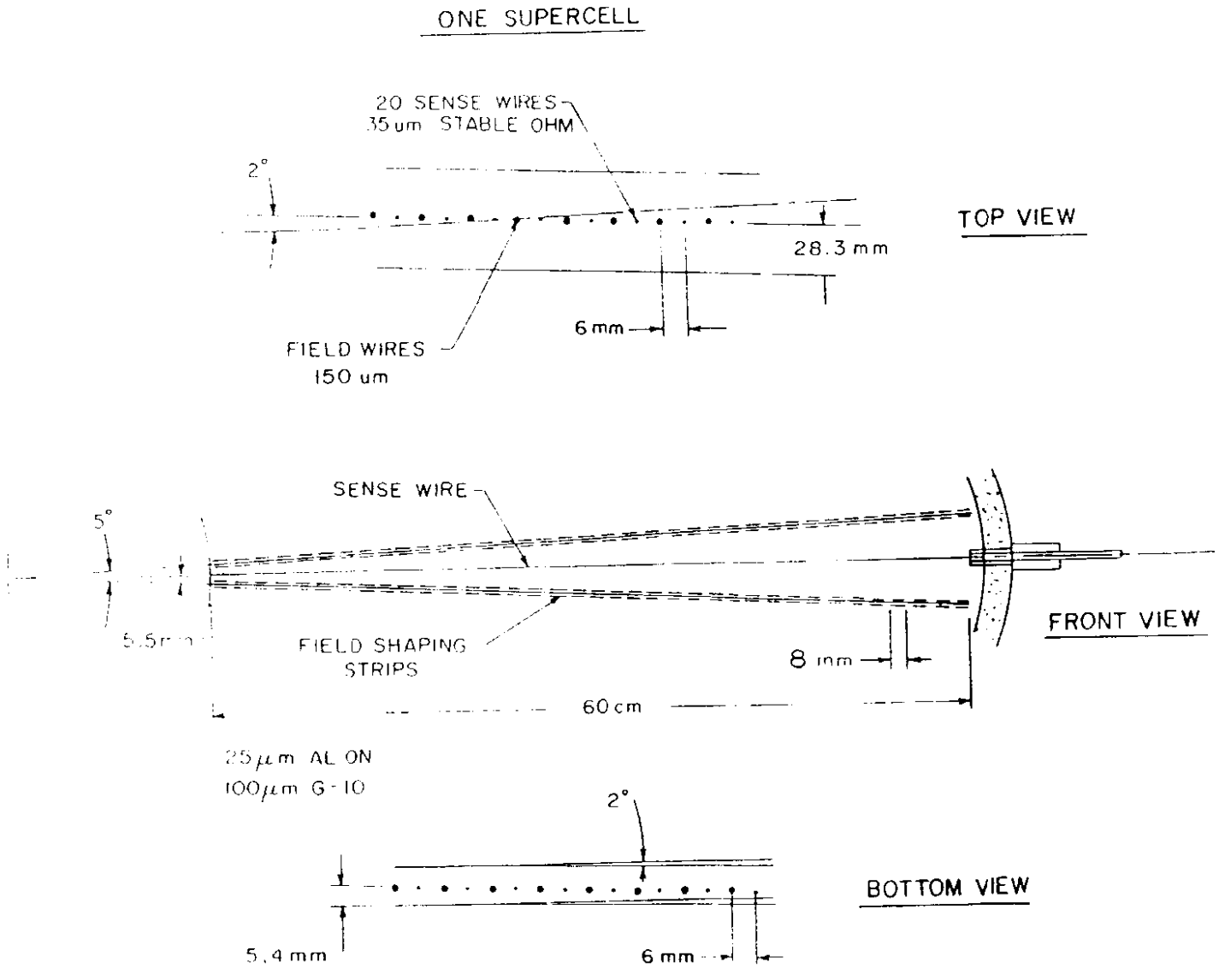
ONE SUPERCELL
20 SENSE WIRES
35 um STABLE OHM
2°
28.3 mm
TOP VIEW
6 mm
FIELD WIRES
150 um
SENSE WIRE
5°
5.5 mm
FIELD SHAPING
STRIPS
8 mm
FRONT VIEW
60 cm
25 μm AL ON
100 μm G-10
2°
5.4 mm
6 mm
BOTTOM VIEW

Fig. 3

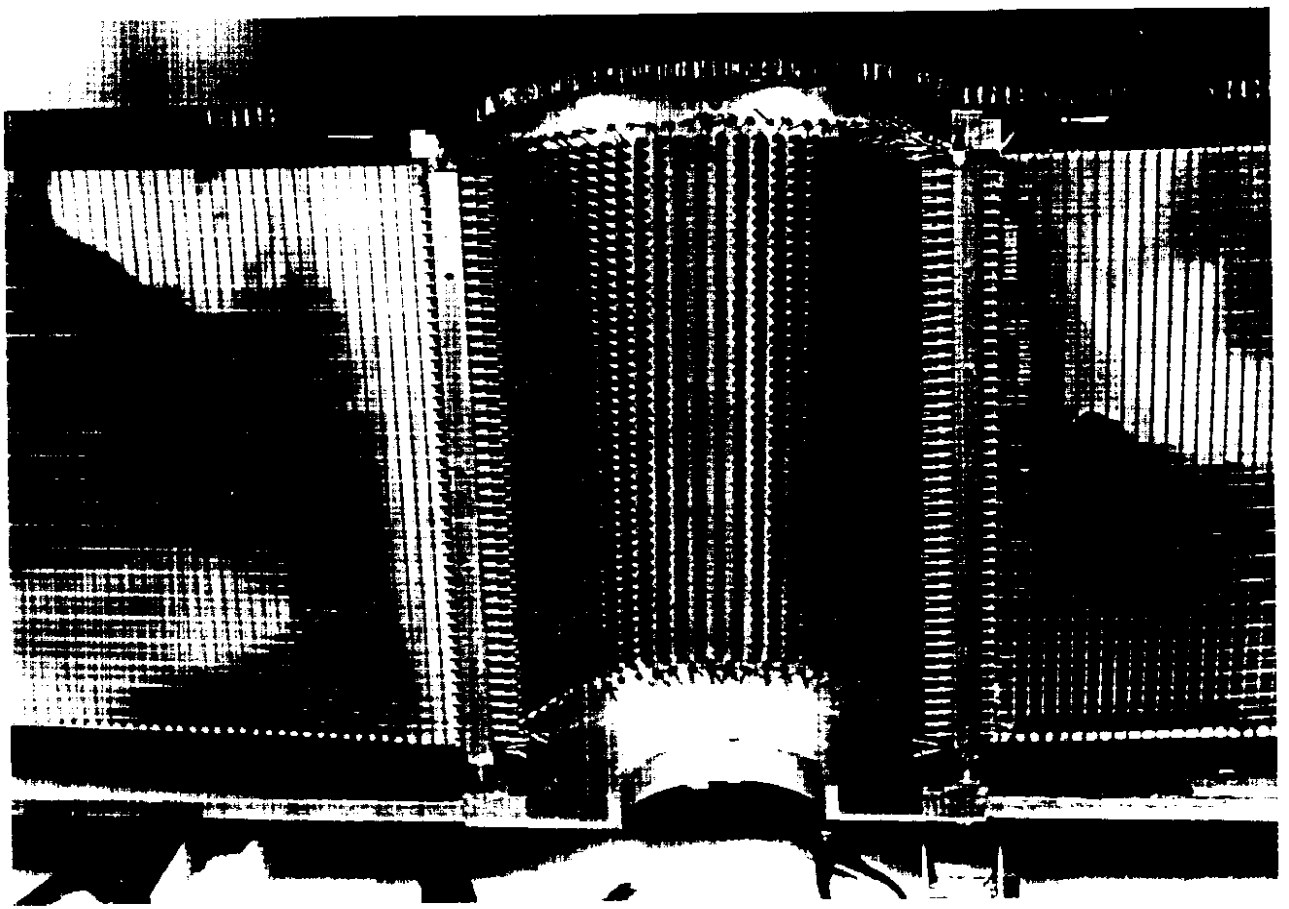

Fig. 4

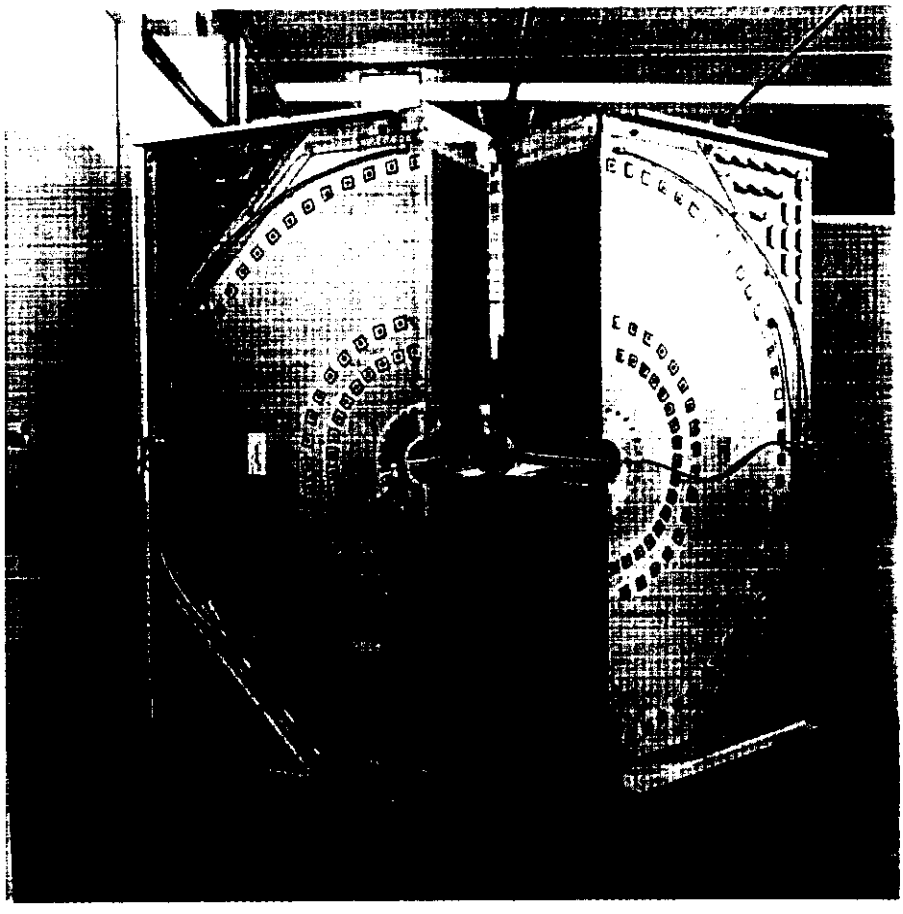

Fig. 5

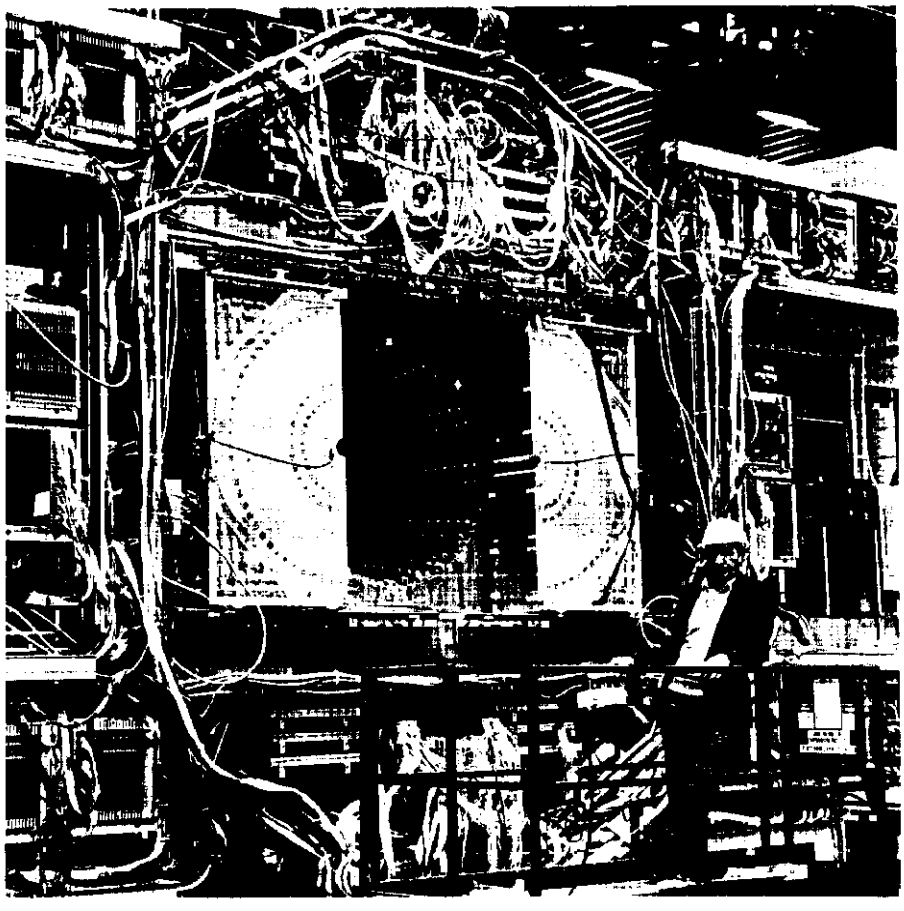

Fig. 6

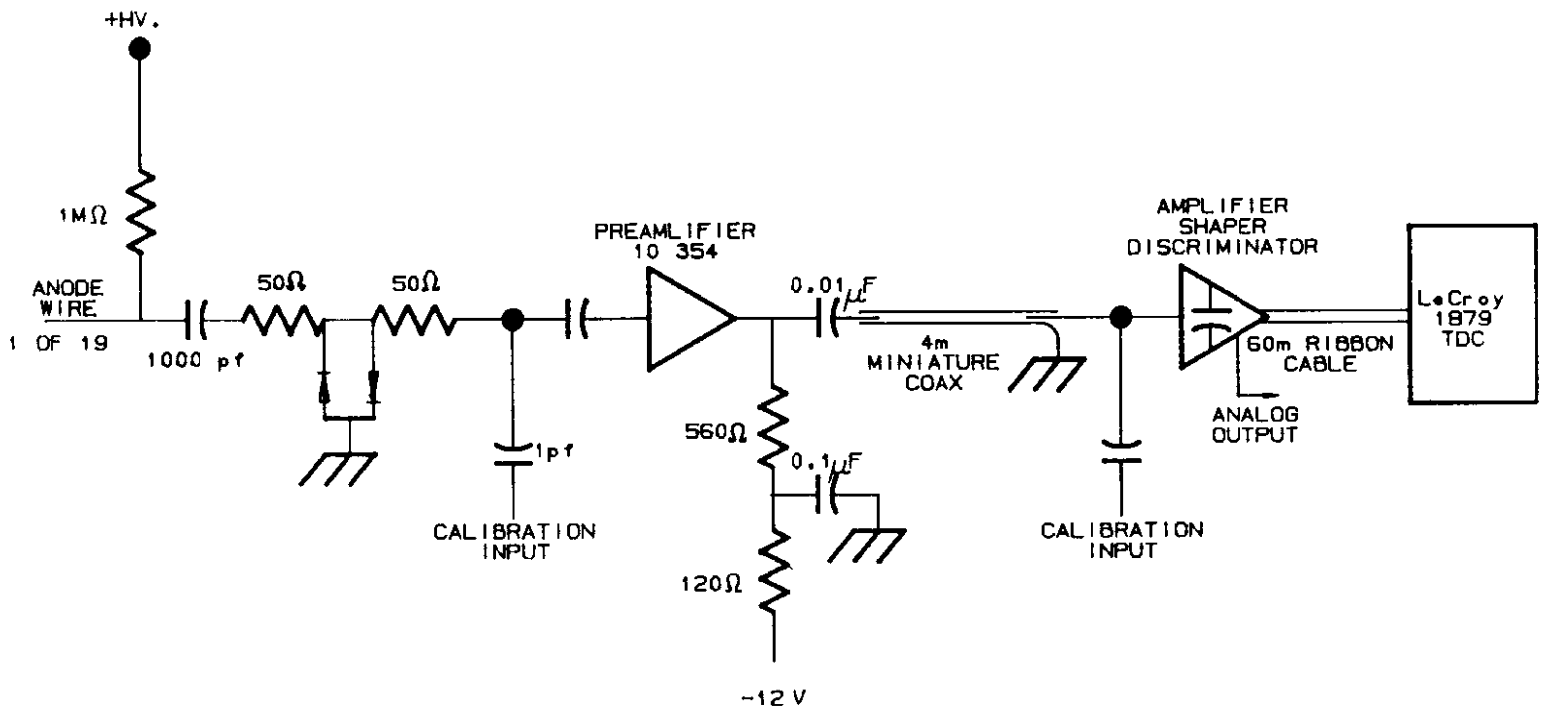
+HV.
1MΩ
ANODE WIRE
1 OF 19
1000 pf
50Ω
50Ω
PREAMLIFIER 10 354
0.01μF
4m MINIATURE COAX
AMPLIFIER SHAPER DISCRIMINATOR
60m RIBBON CABLE
LeCroy 1879 TDC
ANALOG OUTPUT
1pf
CALIBRATION INPUT
560Ω
0.1μF
120Ω
-12 V
CALIBRATION INPUT

Fig. 7

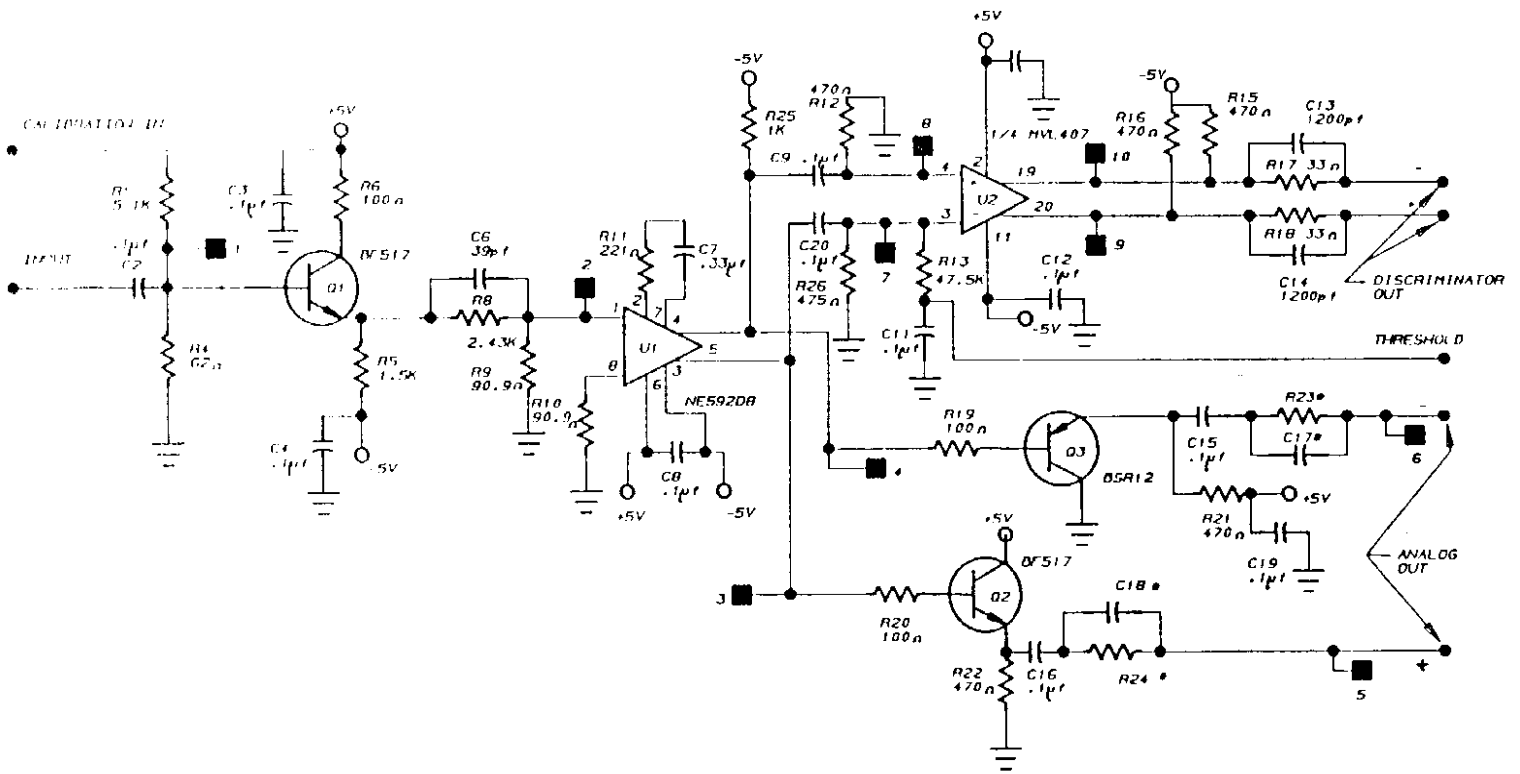
+5V
-5V
R25 1K
470Ω R12
C9 .1μf
1/4 MVL407
R16 470Ω
R15 470Ω
C13 1200pf
R17 33Ω
R18 33Ω
C14 1200pf
DISCRIMINATOR OUT
C20 .1μf
R26 475Ω
R13 47.5K
C12 .1μf
C11 .1μf
THRESHOLD
C6 39pf
R8 2.43K
R9 90.9Ω
R10 90.9Ω
R11 221Ω
C7 .33μf
NE592DB
C8 .1μf
R19 100Ω
Q3
BSR12
R23*
C17*
C15 .1μf
R21 470Ω
C19 .1μf
ANALOG OUT
BF517
Q2
R20 100Ω
C18*
R22 470Ω
C16 .1μf
R24*
R6 100Ω
BF517
Q1
R5 1.5K
C4 .1μf
C3 .1μf
C2
INPUT

Fig. 8

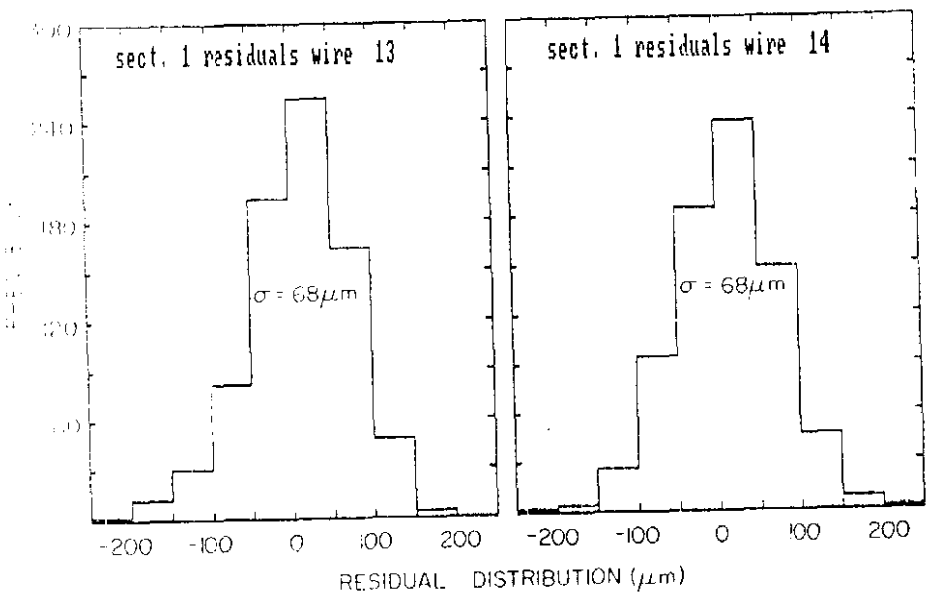
sect. 1 residuals wire 13
σ = 68μm
sect. 1 residuals wire 14
σ = 68μm
-200
-100
0
100
200
-200
-100
0
100
200
RESIDUAL DISTRIBUTION (μm)

Fig. 9

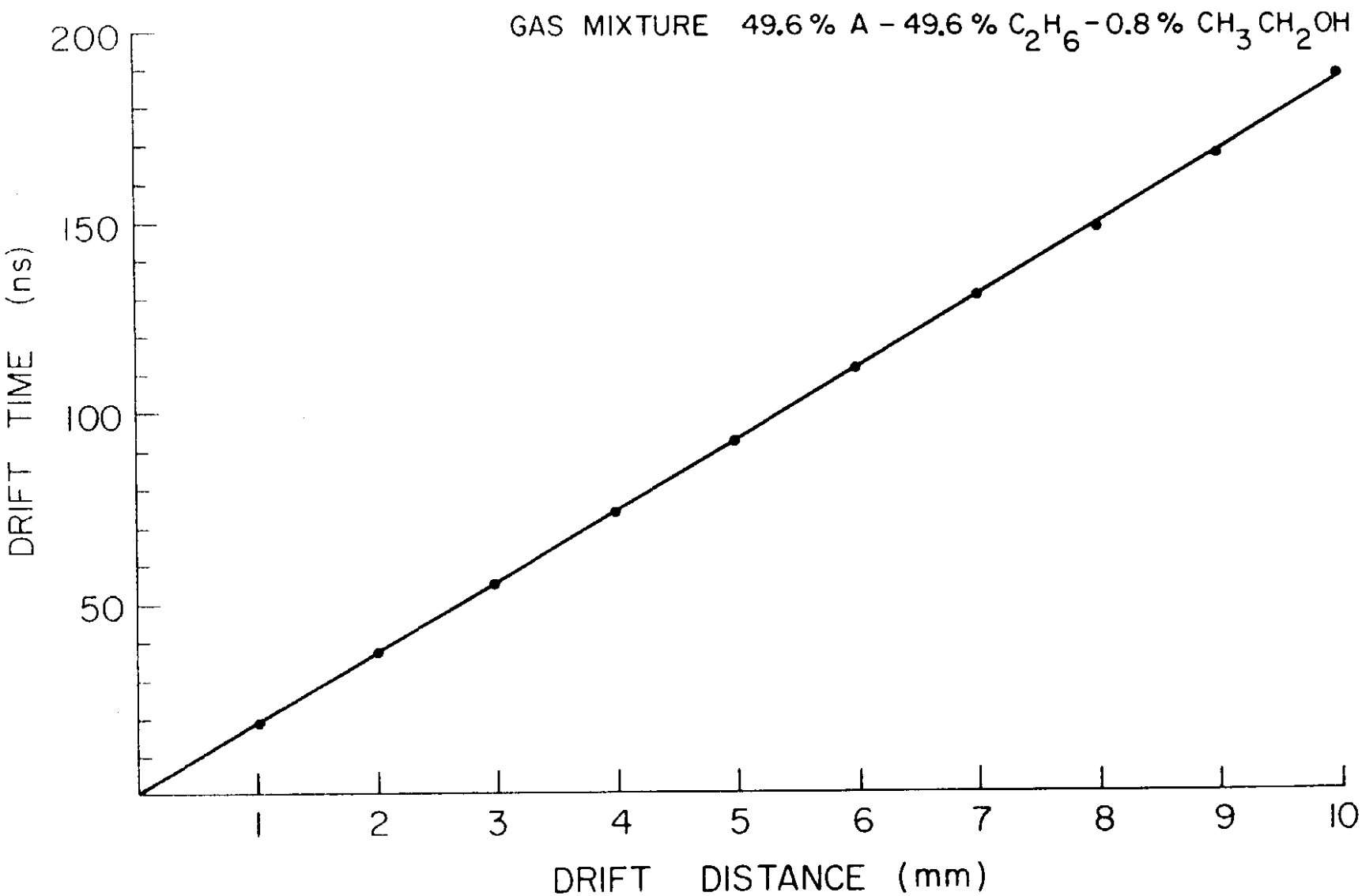
GAS MIXTURE 49.6 % A - 49.6 % C_2H_6 - 0.8 % CH_3CH_2OH
DRIFT TIME (ns)
200
150
100
50
1
2
3
4
5
6
7
8
9
10
DRIFT DISTANCE (mm)

Fig. 10

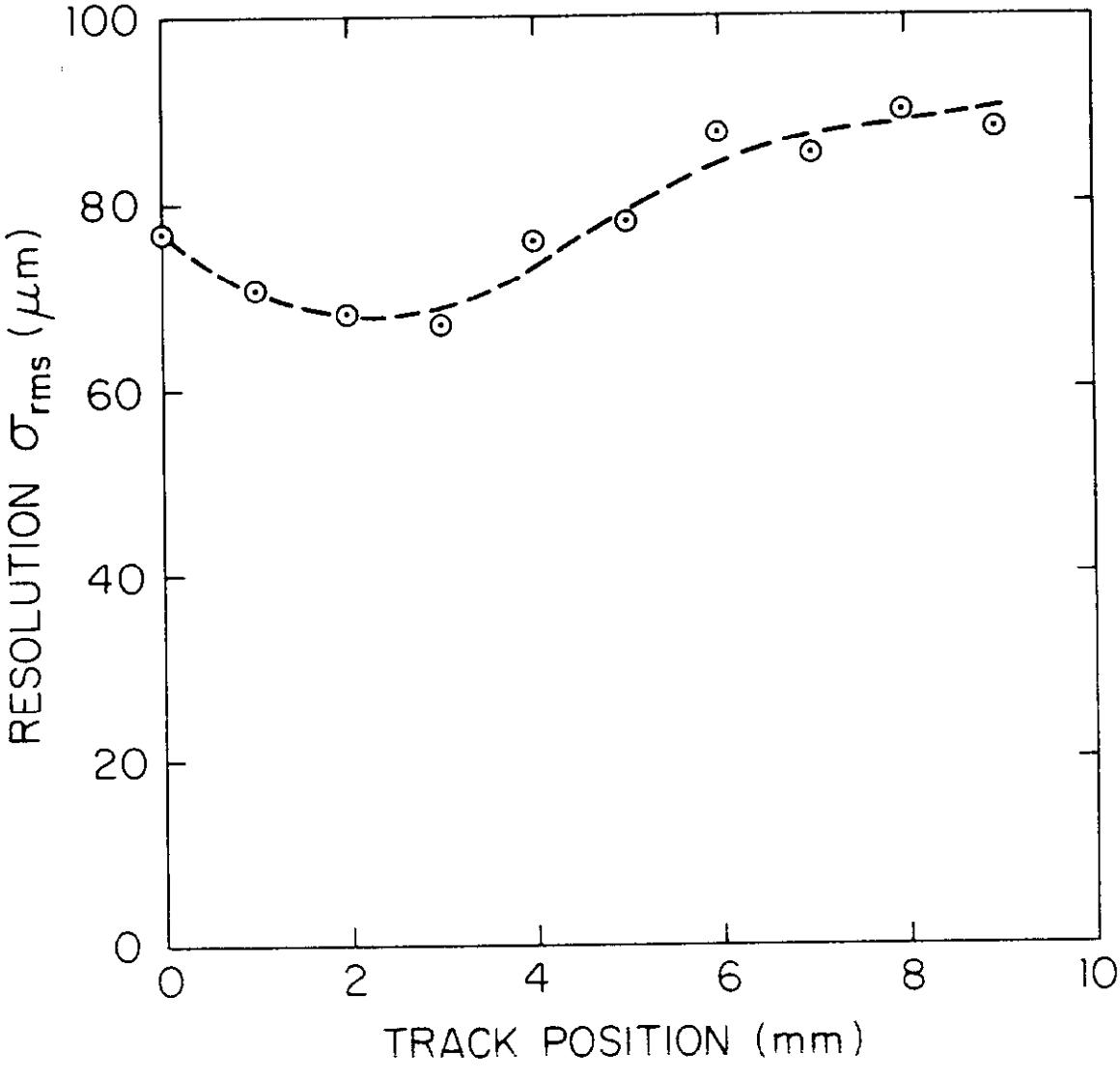
100
80
60
40
20
0
RESOLUTION σ_{rms} (μm)
0
2
4
6
8
10
TRACK POSITION (mm)

Fig. 11

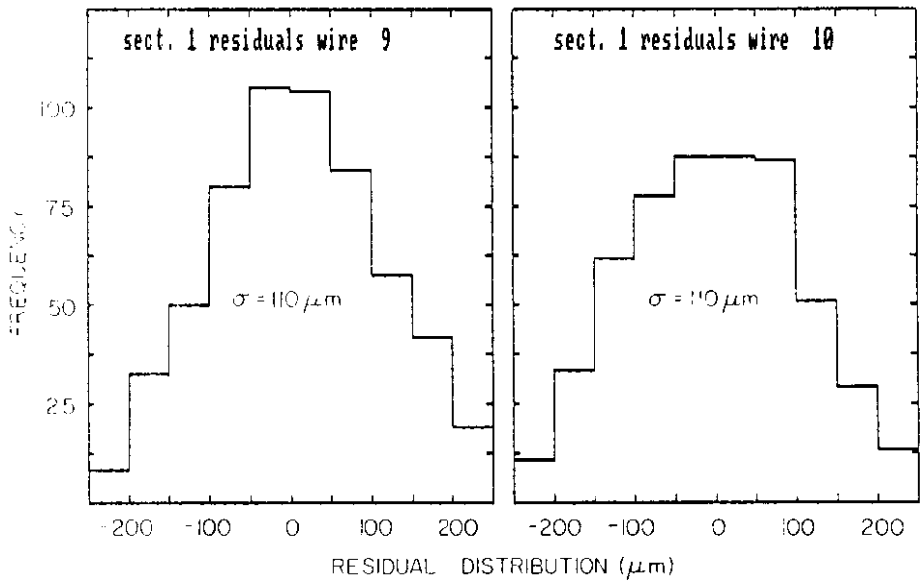
sect. 1 residuals wire 9
sect. 1 residuals wire 10
100
75
50
25
σ = 110 μm
σ = 110 μm
-200
-100
0
100
200
-200
-100
0
100
200
RESIDUAL DISTRIBUTION (μm)

Fig. 12

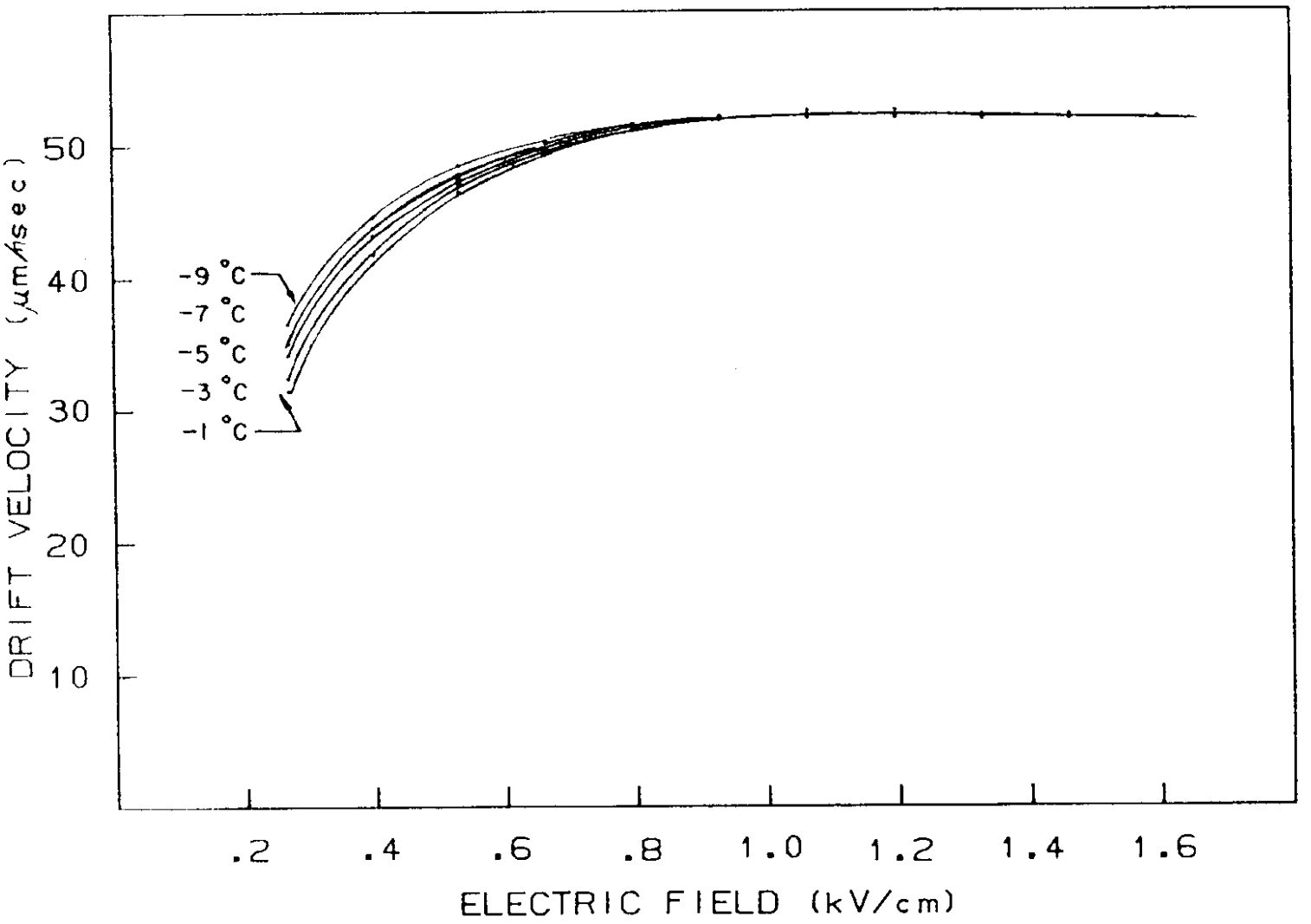
DRIFT VELOCITY (μm/μsec)
50
40
30
20
10
-9 °C
-7 °C
-5 °C
-3 °C
-1 °C
.2
.4
.6
.8
1.0
1.2
1.4
1.6
ELECTRIC FIELD (kV/cm)

Fig. 13

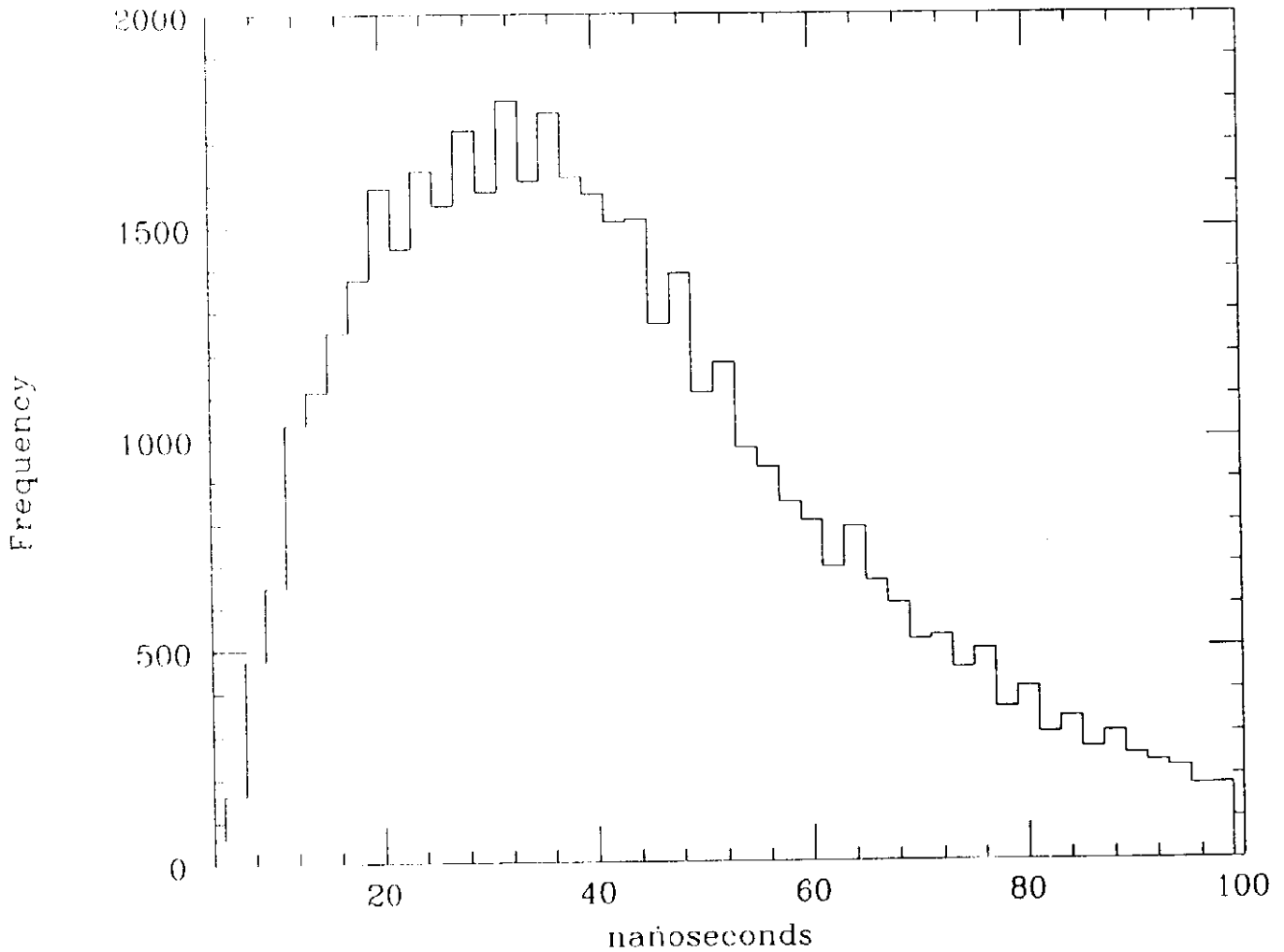

Fig. 14

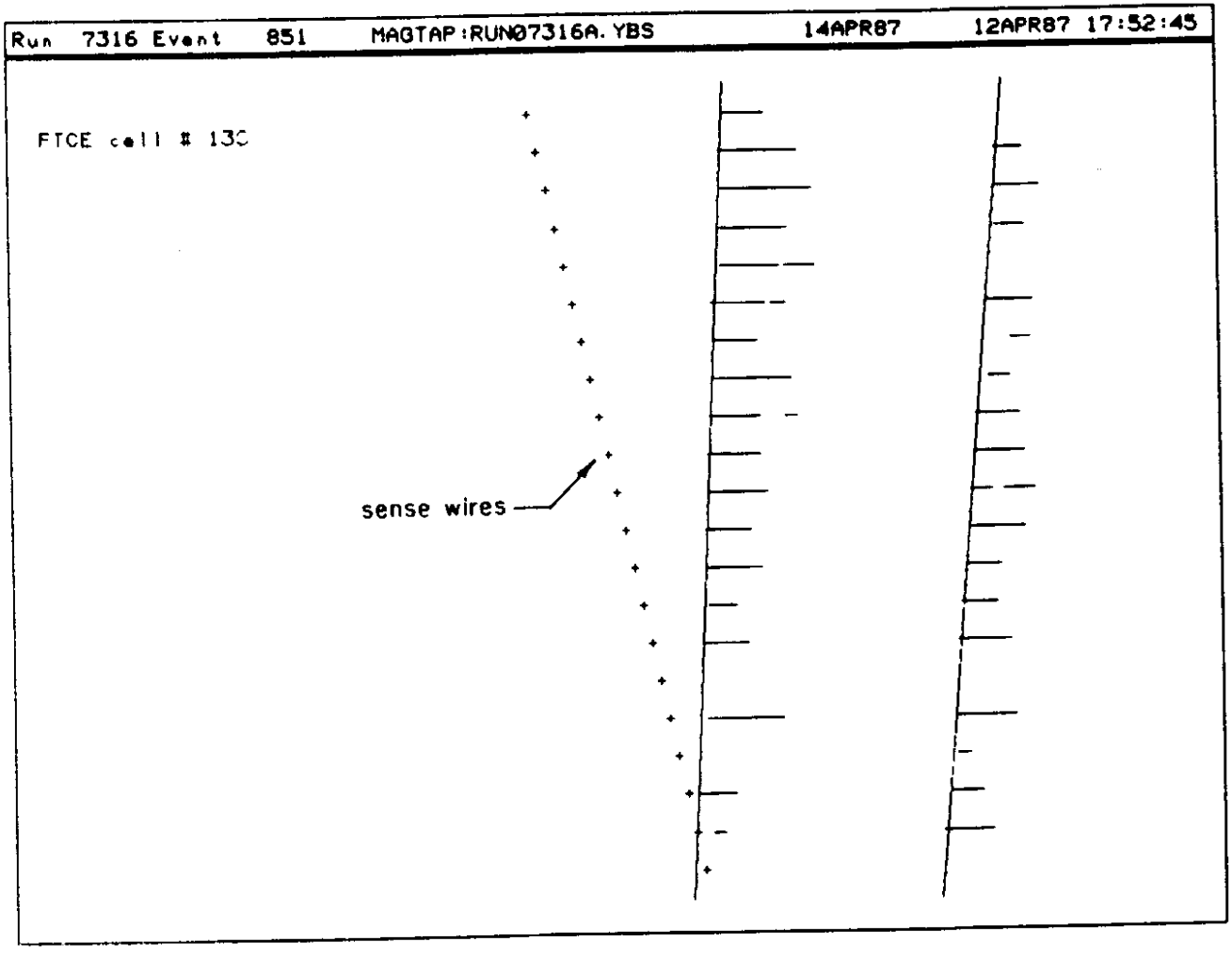
Run 7316 Event 851
MAGTAP:RUN07316A.YBS
14APR87
12APR87 17:52:45
FTCE cell # 130
sense wires

Fig. 15a

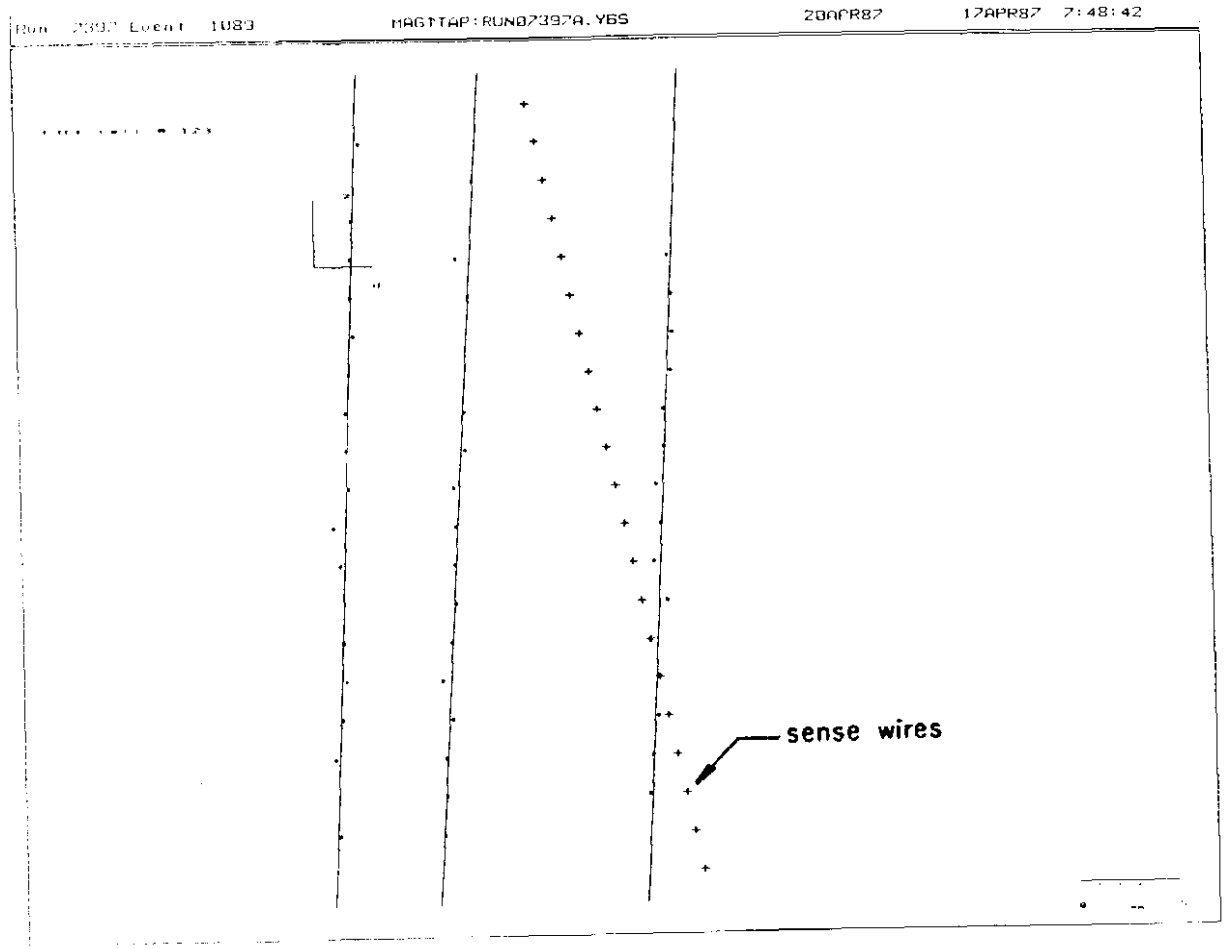

Fig. 15b

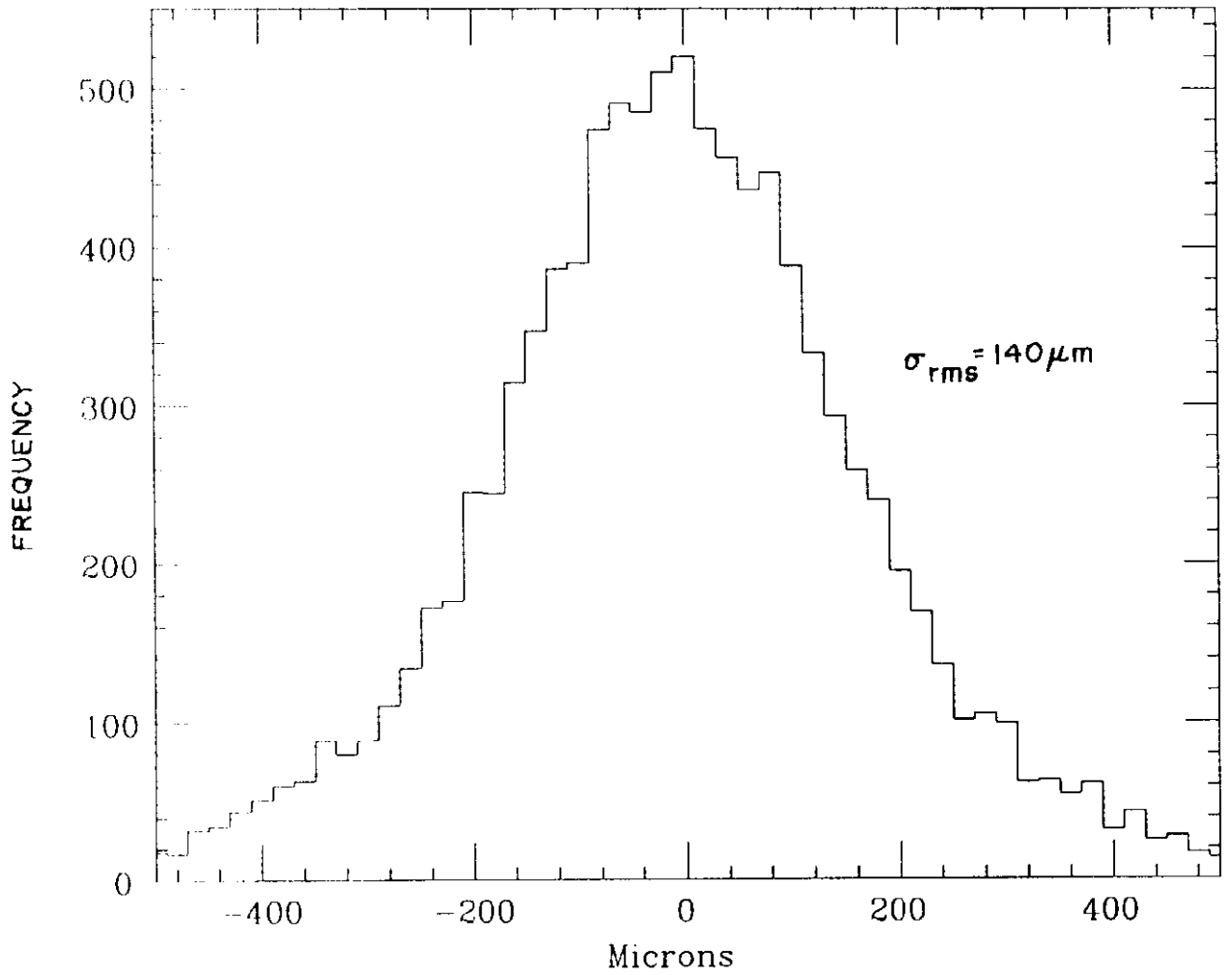
FREQUENCY
500
400
300
200
100
0
-400
-200
0
200
400
Microns
$\sigma_{rms} = 140\mu m$

Fig. 16